Surface and interfacial energies of $CoSi_2$ and Si films: Implications regarding formation of three-dimensional silicon–silicide structures

by K. N. Tu

Formation of three-dimensional, multilevel structures consisting of epitaxial silicon and silicide films is currently of interest in the microelectronics technology. However, such structures have been difficult to produce because of surface wetting differences. To obtain associated surface energy information, an analysis was carried out of published data on the kinetics of crystallization of amorphous $CoSi_2$ and Si films. The analysis indicated that the amorphous-to-crystalline interfacial energy of amorphous $CoSi_2$ films is about one-fourth that of amorphous Si films, from which it was inferred that the surface energy of epitaxial $CoSi_2$ films is less than that of epitaxial Si films. The approach used in the analysis is general and should be extendable to other systems.

Introduction

In order to achieve epitaxial growth of a thin film having the same lattice structure as that of an underlying substrate, it is not only crucial that a close lattice match be achieved at the interface between the film and the substrate, but also that the surface energy of the film be less than or very nearly equal to that of the substrate, because of the principle of minimization of surface energy. If the surface energy of the film is greater than that of the substrate, it tends to agglomerate as it grows, even if there is no lattice misfit. If a planar, epitaxial structure A/B/A/B is to be formed, where A and B are layers of two different types of materials, it would appear at first sight that the principle of minimization of surface energy would need to be violated: If B wets A, A should not wet B but should agglomerate on it. This is shown schematically in **Figure 1**, for which the surface energy σ_s of the substrate is assumed to be appreciably greater than the surface energy σ_o of the overlayer. Thus, it would not appear that planar, epitaxial A/B/A/B structures could be formed from such materials.

Although GaAs–AlGaAs and Si–$Si_{1-x}Ge$ ($x < 0.1$) superlattices can be fabricated [1, 2], such pairs nevertheless consist of very similar materials having nearly identical lattice structures and surface energies. However, for silicon and the silicides, this is not the case. Hence, it is not evident that the formation of planar, epitaxial A/B/A/B silicon–silicide structures should be possible.

A characterization of thin-film growth morphology on a substrate is shown in **Figure 2**, in which the three well-known growth modes are plotted in coordinates of interfacial misfit (horizontal axis) and surface-energy difference between film and substrate (vertical axis) [3]. The terms a_s and a_o are the lattice parameters of the substrate and the film (overlayer), respectively. The three growth modes are 1) the Frank–van der Merwe mode, in which the film grows epitaxially layer by layer; it occurs when the misfit is nearly zero and its surface energy is less than that of the substrate; 2) the Weber–Volmer mode, in which island growth prevails when the surface energy of the substrate is greater than that of the film and in which, during film growth, the wetting angle between the island and the substrate increases with the interfacial misfit; and 3) the Stranski–Krastanov mode, in which a combination of layered and island growth occurs. The dashed line denotes the separation between the latter two modes.

If a planar, epitaxial, multilevel structure consisting of several layers of two or more materials is to be formed (e.g., a superlattice or an A/B/A/B multilevel structure), surface energy and misfit conditions must be met which lie within the small circle at the origin. It should be noted, however, that in selecting dissimilar materials for that purpose, while the misfit is usually known because the lattice parameters of the materials are usually known, the difference in their surface energies is usually *not* known.

Currently, means to achieve the formation of three-dimensional silicon–silicide structures are of considerable interest in the microelectronics technology. This is because of the increasing need for three-dimensional device and interconnection structures in order to further increase circuit density. Many attempts have been made to fabricate structures of Si/$CoSi_2$/Si, Si/$NiSi_2$/Si, or Si/CaF_2/Si [4–6], but most have been only partially successful. Although the silicides $CoSi_2$ and $NiSi_2$ have a cubic CaF_2 crystal structure and a lattice constant which matches that of Si to within 1%, their surface structures differ appreciably from that of Si. And their surface energies are not known.

In forming a Si/$CoSi_2$/Si structure in which the lower portion is a (111) Si surface, it has been found that the $CoSi_2$ layer prefers to grow in a twinning orientation of the (111) Si surface, although Si grows epitaxially on (111) $CoSi_2$ [7]. This asymmetrical growth is indicated in the schematic atomic structure of **Figure 3**. Although the energy associated with the twinning interface is less than that of the epitaxial interface, the latter appears to be preferred for the epitaxial growth of Si on a $CoSi_2$ surface.

In order to develop an understanding of such asymmetrical growth, it would be useful if some measure could be obtained of the surface energies of epitaxial films of Si and $CoSi_2$. Although scanning tunneling microscopy and other surface analysis techniques can be used to

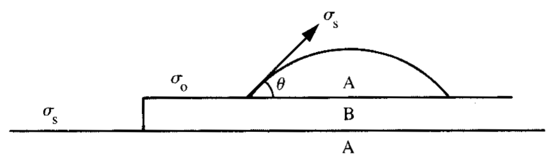

Figure 1

Asymmetrical growth morphology of materials A and B. Illustratively, B wets A, but A does not wet B; it agglomerates onto it.

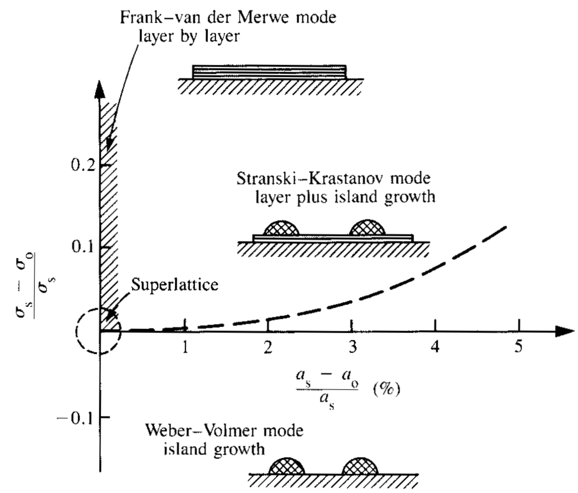

Figure 2

Schematic diagram of the three thin-film growth modes in coordinates of interfacial misfit (horizontal axis) and surface-energy difference between film and substrate (vertical axis). The dashed curve separates the Stranski–Krastanov and the Weber–Volmer modes.

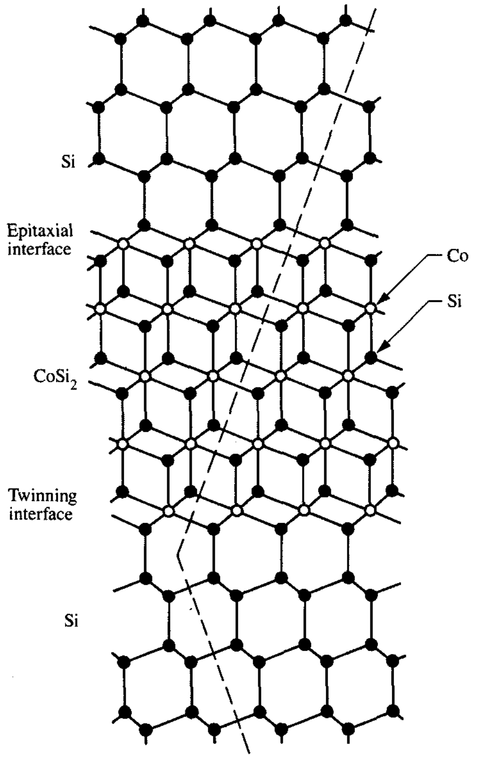

Figure 3

Schematic diagram of atomic structure of Si/$CoSi_2$/Si layered configuration; lower portion corresponds to that of a (111) Si surface. The dashed lines indicate that the $CoSi_2$ film grows in a twinning orientation on the (111) Si surface, but that the Si film (upper layer) grows epitaxially on the $CoSi_2$ film.

determine surface structure and composition, and high-resolution transmission electron microscopy and ion channeling to determine interface structure and composition, none of these methods are suitable for determining surface energy.

This paper describes a method for obtaining the amorphous-to-crystalline interfacial energies of amorphous $CoSi_2$ and Si films, by an analysis of their kinetics of crystallization, and by inference, some approximate information regarding the *surface* energies of *epitaxial* films of those materials. The method is general and should therefore be extendable to other systems.

Analysis method

For both amorphous Si and $CoSi_2$ films, crystallization is a first-order phase transition which proceeds by nucleation and growth. Assuming that the nucleation is random and constant, and that the growth is isotropic and constant, the transition can be described by the equation of Johnson, Mehl, and Avrami [8–10], viz.,

$$X_T = 1 - \exp(-X_{ext}), \tag{1}$$

where X_T and X_{ext} are defined as the fraction of the transformed volume and fraction of the extended volume, respectively. The latter is given by

$$X_{ext} = \int_{\tau=0}^{\tau=t} \frac{4\pi}{3} IG^3(t-\tau)^3 d\tau, \tag{2}$$

where I is the nucleation rate, G is the growth rate, and t is the time of transformation. Hence, if the nucleation and growth rates can be determined, X_{ext} can be obtained from Equation (2), and subsequently X_T can be obtained from Equation (1). Alternatively, for a thin film, X_T can be measured (during transformation) directly by an imaging technique or indirectly, e.g., from the change in its resistivity.

If the nucleation is random, continuous, and proceeds at a constant rate, and the growth is isotropic in three dimensions and linear with time, Equation (2) reduces to

$$X_{ext} = \frac{\pi}{3} IG^3t^4. \tag{3}$$

Thus, Equation (1) becomes

$$X_T = 1 - \exp(-Kt^4), \tag{4}$$

where

$$K = \frac{\pi}{3} IG^3 = \frac{\pi}{3} I_0G_0^3 \exp\left(-\frac{\Delta H_N + 3\Delta H_G}{kT}\right). \tag{5}$$

The nucleation and growth rates have been assumed to be characterized by Boltzmann distributions, viz.,

$$I = I_0 \exp\left(\frac{-\Delta H_N}{kT}\right) \tag{6}$$

and

$$G = G_0 \exp\left(\frac{-\Delta H_G}{kT}\right). \tag{7}$$

The terms ΔH_N and ΔH_G are respectively the activation enthalpies of nucleation and growth.

Experimentally, X_T is measured as a function of time and temperature, and a constant value is chosen in order to obtain the activation enthalpy of transformation. If we choose, e.g., $X_T = 0.5$, Equation (4) gives

$$Kt^4 = constant. \tag{8}$$

By taking the logarithm of Equation (8), we obtain

$$-\frac{\Delta H_N + 3\Delta H_G}{kT} + 4 \ln t = constant. \tag{9}$$

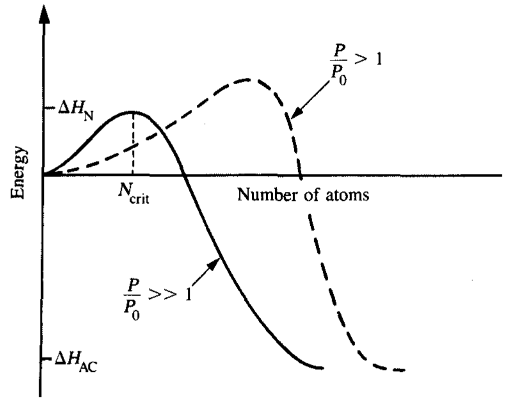

Figure 4

Schematic curves depicting nucleation behavior.

The slope of a plot of ln t vs. $1/kT$ gives the activation enthalpy of transformation, $(\Delta H_N + 3\Delta H_G)/4$, thus making it possible to obtain ΔH_N by measuring ΔH_G, and vice versa. Given ΔH_N, it is possible to estimate the amorphous-to-crystalline interfacial energy by using classical nucleation theory [11].

Figure 4 shows schematic curves depicting nucleation behavior in which an activation energy is required in order to form a critical nucleus containing N_{crit} atoms, where ΔH_N is the associated energy required, ΔH_{AC} is the heat of crystallization, and the pressure ratio P/P_0 is a measure of the supersaturation or degree of departure from equilibrium.

Following classical nucleation theory, formation of a nucleus containing N atoms requires an energy

$$\Delta H_N = -aN\Delta H_{AC} + bN^{2/3}\sigma_{AC} , \tag{10}$$

where σ_{AC} is the amorphous-to-crystalline interfacial energy and a and b are geometrical shape factors. For the critical nucleus,

$$\frac{\partial \Delta H_N}{\partial N} = 0.$$

Hence,

$$\Delta H_N = \left[a\left(\frac{2b}{3a}\right)^3 + b\left(\frac{2b}{3a}\right)^2\right]\frac{\sigma^3_{AC}}{\Delta H^2_{AC}} \tag{11}$$

and

$$N_{crit} = \left(\frac{2b}{3a}\right)^3\left(\frac{\sigma_{AC}}{\Delta H_{AC}}\right)^3. \tag{12}$$

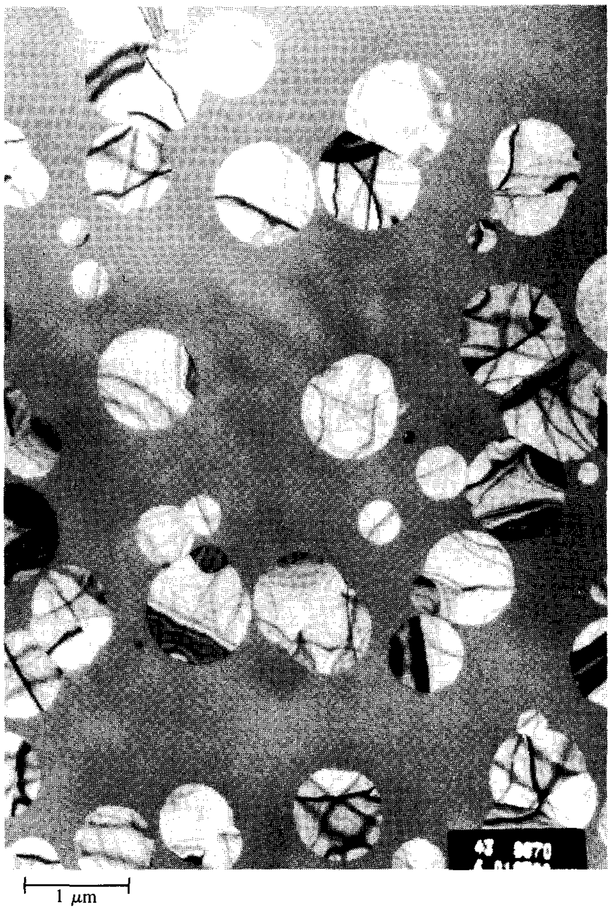

Figure 5

Bright-field transmission electron micrograph of a partially transformed amorphous $CoSi_2$ film, at 150°C. The largest circular grains are about 1 μm in diameter. From [12], reproduced with permission.

Equation (11) makes it possible to calculate σ_{AC} provided that ΔH_{AC}, a, and b are known; ΔH_{AC} can be measured by calorimetry, and a and b can be calculated by assuming that the volume of the nucleus is $N\Omega$, where Ω is the atomic volume. We assume that the nucleation of the crystalline phase occurs at the surface of the amorphous phase, and that the same geometrical shape factors are applicable for $CoSi_2$ and Si.

Crystallization of amorphous $CoSi_2$ films

The crystallization of amorphous $CoSi_2$ films has been examined experimentally [12] using films prepared by vacuum deposition onto oxidized silicon wafers. **Figure 5** shows a bright-field transmission electron micrograph of a partially transformed amorphous $CoSi_2$ film, obtained at 150°C [12]. The circular images are from grains of crystalline $CoSi_2$. Their distribution is random and their

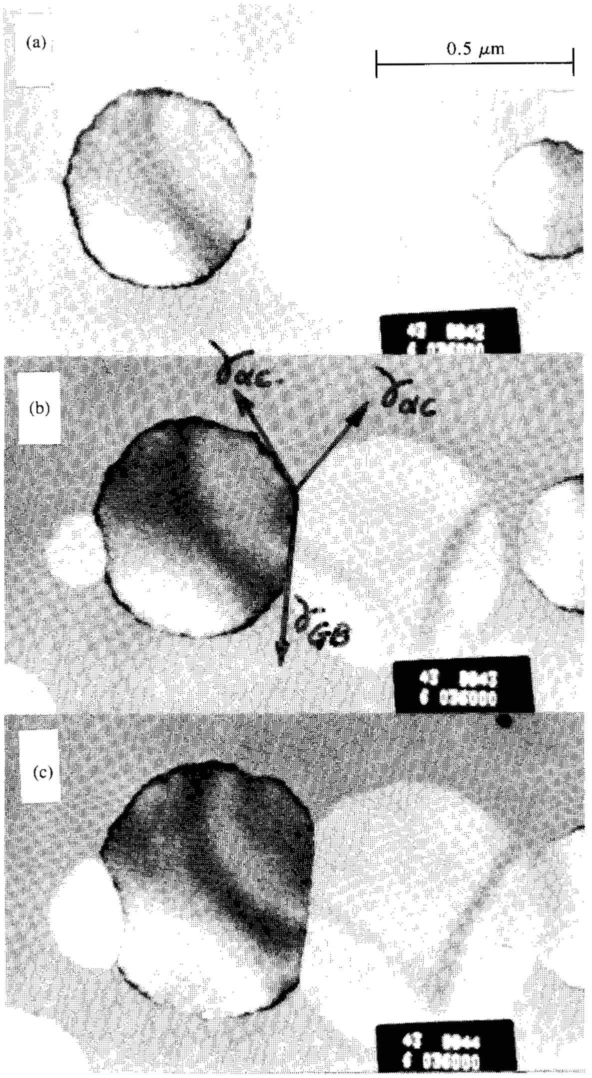

Figure 6

Sequential growth of adjacent circular $CoSi_2$ grains, and the formation of grain boundaries between impinging grains. From [12], reproduced with permission.

bend contours show that each is a single crystal without preferred orientation. Nucleation occurs independently and randomly in time and space. **Figure 6** shows the sequential growth of several circular grains and the formation of grain boundaries between impinging grains. The growth is isotropic, as indicated by the observation that the shape of the grains remains circular during growth. By measuring the diameters of the grains as a function of time, the growth rate can be determined and is found to be constant. Since the number of circular grains in a given area can be obtained as a function of time and temperature, the nucleation rate can be calculated.

Because the nucleation and growth of an amorphous $CoSi_2$ film satisfy the conditions described by the phase transformation model of Johnson, Mehl, and Avrami, Equation (1) can be applied to its amorphous-to-crystalline transformation. **Figure 7** shows two plots of resistivity changes of an amorphous $CoSi_2$ film in van der Pauw's geometry that was ramp-annealed at 0.5°C/min and 3°C/min in a He furnace, from room temperature to 500°C. The resistivity changes obtained *in situ* show that the amorphous-to-crystalline transformation occurs around 150°C [13]. **Figure 8** shows the change in the fraction of the transformed volume upon annealing at four temperatures in the vicinity of 150°C. The changes are expressed in terms of the resistivities ρ_a, ρ_c, and $\rho(t)$ in the amorphous and crystalline states and at a time t, respectively. The intercepts with the dashed horizontal line are taken as measures of corresponding annealing times. Using these data and Equation (9), the activation energy of the amorphous-to-crystalline transformation of the $CoSi_2$ film is found to be

$$\Delta H_T = \frac{\Delta H_N + 3\Delta H_G}{4} = 0.9 \text{ eV}. \qquad (13)$$

As discussed above, the nucleation rate can be calculated from the measured increase in the number of grains in a given area, and the growth rate can be obtained from the measured increase in grain diameter. Since the latter can be used to obtain ΔH_G, it follows that ΔH_T, ΔH_N, and ΔH_G can be obtained independently, and that it should be possible to check self-consistency by means of Equation (13). However, we choose to obtain ΔH_N from that equation, using measured values of ΔH_T and ΔH_G in order to more effectively compare (in the following section) the crystallization behavior of amorphous $CoSi_2$ films with that of amorphous Si films. (It has not yet been possible to obtain an independent measurement of ΔH_N for amorphous Si films. Hence, for the purpose of that comparison, we choose to obtain ΔH_N from measurements of ΔH_T and ΔH_G.)

It has been found that ΔH_G is 1.1 eV for amorphous $CoSi_2$ films [14]. Using that value in Equation (13) gives $\Delta H_N = 0.3$ eV. The heat of crystallization ΔH_{AC} of amorphous $CoSi_2$ has been found to be 0.05 eV/atom*. Using the above values in Equations (11) and (12) gives $\sigma_{AC} = 0.09$ eV/cm^2 (or 160 erg/cm^2) and $N_{crit} \sim 8$ atoms.

Comparison with Si films

Crystallization of amorphous Si has been widely studied and is covered by a large body of literature. The epitaxial

*L. T. Shi and K. N. Tu, IBM Thomas J. Watson Research Center, Yorktown Heights, NY, unpublished.

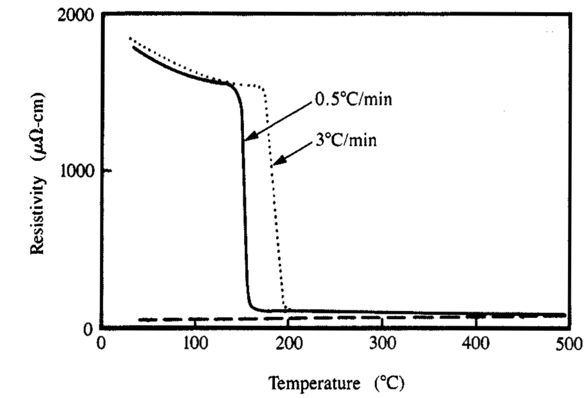

Figure 7

Resistivity changes of an amorphous $CoSi_2$ film in van der Pauw's geometry, upon ramp-annealing in a He furnace from room temperature to 500°C, at 0.5°C/min and 3°C/min. From [13], reproduced with permission.

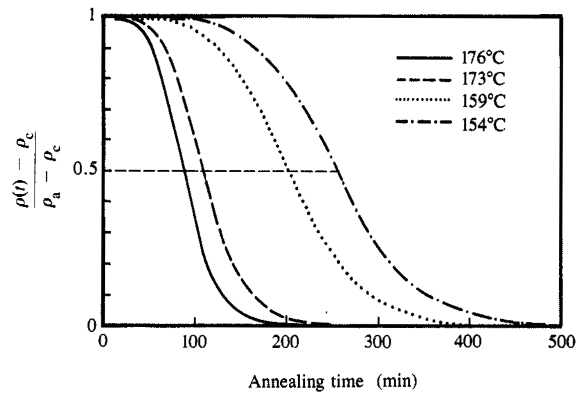

Figure 8

Effect of annealing on the fraction of the transformed volume of an amorphous $CoSi_2$ film, expressed in terms of its resistivity at time t and in its amorphous and crystalline states. From [13], reproduced with permission.

growth of amorphous Si on a single-crystal Si surface has been a subject of considerable interest. For example, ion implantation can be used to transform the surface of a Si wafer into amorphous Si. By subsequent rapid laser annealing or slow furnace annealing, the amorphous Si can be converted back to epitaxial, crystalline Si. Amorphous Si can also be formed by MBE (molecular beam epitaxy) deposition. In the case of crystallization on a single-crystal Si surface, nucleation is not required. On the other hand, crystallization of an amorphous Si film on an oxidized Si wafer requires both nucleation and growth. Thus, comparison of the two processes makes it possible to separate out effects due to nucleation and growth.

The study of epitaxial crystallization of amorphous Si films on single-crystal surfaces was pioneered by Mayer and his associates [15] using ion-beam channeling techniques. Refinement of the kinetics of epitaxial growth was carried out by Olson and Roth by using time-resolved reflectivity [16].

Values of the parameters ΔH_N, σ_{AC}, and N_{crit} for amorphous Si films were calculated following the approach described above for amorphous $CoSi_2$ films. **Table 1** contains a summary of the values of the measured and calculated parameters. As can be seen, the amorphous-to-crystalline interfacial energy for amorphous $CoSi_2$ films was found to be one-fourth that of amorphous Si films. The number of atoms in the critical nucleus of amorphous Si films was found to be about 64 atoms. This number seems reasonable, since amorphous Si displays short-range

Table 1 Measured and calculated parameters for amorphous $CoSi_2$ and Si films. Measured values are from cited references.

Parameters	$CoSi_2$	*Si*
ΔH_T	0.9 eV [13]	3.4 eV [15]
ΔH_G	1.1 eV [14]	2.7 eV [15]
ΔH_{AC}	0.05 eV/atom*	0.1 eV/atom [15]
ΔH_N	0.3 eV	5.5 eV
σ_{AC}	0.09 eV/cm^2	0.4 eV/cm^2
N_{crit}	~8 atoms	~64 atoms

*L. T. Shi and K. N. Tu, IBM Thomas J. Watson Research Center, Yorktown Heights, NY, unpublished.

order; its nearest neighbors are the same as those in crystalline Si; and the critical nucleus must involve second- or third-nearest neighbors.

It is important to note that although the measured values in the table are quite reliable for calculating σ_{AC} and N_{crit}, the geometrical shape factors are uncertain because shapes must be assumed for the nuclei. For this reason, the calculated values of σ_{AC} and N_{crit} are reasonable for the purpose of comparison between $CoSi_2$ and Si films, but their absolute values should be taken with caution. In addition, the σ_{AC} values of the critical nuclei of the films may not be the same as those for the corresponding bulk materials because the critical nuclei of the films consist of very small clusters of atoms.

In principle, it should be possible to estimate the surface energies of epitaxial $CoSi_2$ and Si films from their σ_{AC} values by 1) determining the grain boundary energy from the sine law obeyed by the surface tensions of adjacent grains in equilibrium with each other at their triple point [e.g., see Figure 6(b)] and 2) subsequently determining the surface energy by assuming extension of the grain boundaries to the surface. Accordingly, we infer that the trend is most likely that indicated by their σ_{AC} values; viz., that the surface energy of an epitaxial $CoSi_2$ film is less than that of an epitaxial Si film. Formation of epitaxial, multilevel configurations of the two types of films may therefore require that means be used to offset this, for example by the use of impurities or alloying additions.

In reference to Figure 2, it should be noted that the equivalence

$$\frac{\sigma_s - \sigma_0}{\sigma_0} = \frac{\sigma_s}{\sigma_0} - 1 \tag{14}$$

suggests that by measuring the wetting angle of Si on the surface of $CoSi_2$, it should be possible to obtain the ratio σ_s/σ_0 of the surface energies of the overlayer and substrate without carrying out the analysis presented above. However, that is not practical because the melting point of Si is higher than that of $CoSi_2$.

Summary

An analysis of published data on the kinetics of crystallization of amorphous $CoSi_2$ and Si films has been used to determine their amorphous-to-crystalline interfacial energy. Its magnitude for amorphous $CoSi_2$ films was found to be about one-fourth that of amorphous Si films, suggesting that the surface energy of epitaxial $CoSi_2$ films is less than that of epitaxial Si films. Formation of multilevel, three-dimensional, epitaxial structures from such films of the two materials may therefore require the use of means to increase the surface energy of the $CoSi_2$ films and/or decrease that of the Si films; possibly, e.g., by the use of impurities or alloying additions.

Acknowledgments

The author would like to thank A. Cros (University of Marseilles, France), D. A. Smith (Thomas J. Watson Research Center), and B. Z. Weiss (Technion, Israel), for their cooperation in the study of $CoSi_2$, and members of the Central Scientific Department of the Thomas J. Watson Research Center for depositing the films used in this study.

References

1. *The Technology and Physics of Molecular Beam Epitaxy*, E. H. C. Parker, Ed., Plenum Press, New York, 1985.
2. E. Kasper and J. C. Bean, *Silicon–Molecular Beam Epitaxy*, Vols. I and II, CRC Press, Boca Raton, FL, 1988.
3. M. H. Grabow and G. H. Gilmer, *Surf. Sci.* **194**, 333 (1988).
4. J. C. Hensel, A. F. J. Levi, R. T. Tung, and J. M. Gibson, *Appl. Phys. Lett.* **47**, 151 (1985).
5. E. Rosencher, S. Delage, Y. Campidelli, and F. Arnaud d'Avitaya, *Electron. Lett.* **20**, 762 (1984).
6. E. L. Hall, N. Lewis, B. D. Hunt, and L. J. Schowalter, *Norelco Reporter* **33**, 1 (1986).
7. H. von Kanel, J. Henz, M. Ospelt, J. Hugi, E. Muller, and N. Onda, *Proceedings of the 4th International MBE Conference*, Strasbourg, France, 1989.
8. W. A. Johnson and R. F. Mehl, *Trans. AIME* **135**, 416 (1939).
9. M. Avrami, *J. Chem. Phys.* **8**, 212 (1940); **9**, 177 (1941).
10. J. W. Christian, *Theory of Phase Transformation in Metals and Alloys*, Pergamon Press, New York, 1965.
11. D. Turnbull, *Solid State Phys.* **3**, 226 (1956).
12. K. N. Tu, D. A. Smith, and B. Z. Weiss, *Phys. Rev. B* **36**, 8948 (1987).
13. A. Cros, K. N. Tu, D. A. Smith, and B. Z. Weiss, *Appl. Phys. Lett.* **52**, 1311 (1988).
14. D. A. Smith, K. N. Tu, and B. Z. Weiss, *Ultramicrosc.* **30**, 90 (1989).
15. L. Csepregi, J. W. Mayer, and T. W. Sigmon, *Appl. Phys. Lett.* **29**, 92 (1976).
16. G. L. Olson and J. A. Roth, *Mater. Sci. Rep.* **3**, No. 1, (1988).

Received May 1, 1990; accepted for publication August 27, 1990

King-Ning Tu *IBM Research Division, Thomas J. Watson Research Center, P.O. Box 218, Yorktown Heights, New York 10598.* Dr. Tu is a Research Staff Member and manages the Structure Research Group in the Physical Sciences Department. He received his Ph.D. degree in applied physics from Harvard University in 1968, and subsequently joined IBM at the Thomas J. Watson Research Center. In 1975, he spent a one-year sabbatical leave at the Cavendish Laboratory at Cambridge University, England. Dr. Tu is a Fellow of the American Physical Society and the Metallurgical Society. He received the 1988 Application to Practice Award of the Metallurgical Society. He is currently an Adjunct Professor in the Department of Materials Science at Cornell University and a principal editor of the *Journal of Materials Research*.